Elliptical Core Multimode Fibers for Reduced DSP Complexity in Coherent Optical Transmission

Rekha Yadav, *Graduate Student Member, IEEE*, Fabio A. Barbosa, *Member, IEEE, Member, Optica*, Ming-Jun Li, *Fellow, IEEE, Fellow, Optica,* and Filipe M. Ferreira, *Senior Member, IEEE, Member, Optica*

***Abstract*—In this paper, we analyze the performance of elliptical core graded index fibers with a cladding trench, focusing on a wide range of ovality values and supporting up to 90-polarization modes. We demonstrate a six-fold reduction in the intra-mode group delay and an 11 dB decrease in intra-mode group crosstalk for a 10 km long fiber supporting 90-polarization modes (45 spatial modes), with a fiber crosstalk strength of - 20 dB/km. These fibers maintain the stable inter-mode group properties, same as the fibers optimized for low differential mode group delay. Further suppression of intra-mode group crosstalk strength is achieved in fibers with fewer supported modes and lower coupling strengths. Additionally, we show a 1.89-fold reduction in receiver equalization complexity to achieve the signal-to-noise ratio of 28 dB in 32 GBd 16-QAM data transmission over 10 km by selecting the worst interferers as inputs to the equalizer determined from the channel matrix, compared to circular fibers. We compare the results of using the worst interferers algorithm to the standard mode group division multiplexing scenario of employing the MIMO for a given mode of the size of mode group and shows the improvement in signal-to-noise ratio for a 6 dB at a given complexity using the worst interferers algorithm. We also propose using modes with minimum interferers determined from the channel matrix for the transmission over the same channel, further enhancing throughput whilst reducing receiver complexity. These findings underscore the potential of elliptical core fibers for space-division multiplexed transmission, offering both improved performance and reduced system complexity.**

***Index Terms*— Space-division multiplexing, multi-mode fiber, linear mode coupling, elliptical core fiber, mode group division multiplexing, data-center networks.**

I. Introduction

The continuously increasing traffic within and between datacenters necessitates the scaling of the data rates while reducing the cabling footprint. Multimode fiber (MMF) based space-division multiplexing (SDM) is one of the promising technologies due to its linear scalability of the capacity whilst reducing the cabling footprint compared to *M*-single mode fibers [1-4]. Additionally, the availability of supporting infrastructure, including optoelectronic devices and ASICs, which can be manufactured using conventional processes, enhances its practicality for future systems [5]. In multimode fiber-based SDM, where *M* represents the number of spatial modes utilized, the capacity increases by approximately *M* times compared to the single-mode fiber [6]. Before deploying any new technologies, especially those requiring hardware changes, it is essential to investigate their performance. Accurate modelling and modal analysis are crucial for the effective deployment of these technologies [7].

Several works have investigated the modal analysis and digital signal processing (DSP) requirements at the receiver for circular MMFs [7-11]. The DSP complexity in these fibers scales with the number of spatial modes *M* and delay spread due to the interplay between linear mode coupling and total time spread [12]. To reduce DSP complexity, various fiber designs have been explored including MMFs with optimized graded index core [13] and mode group division multiplexing (MGDM) which exploits a subset of supported modes transmission in the fiber [14-16]. Transmission using principal modes, in which first-order dispersion is independent of frequency, reduces dispersion and coupling, has also been investigated to simplify DSP in weak-to-intermediate coupling graded index core fibers [17-19]. Additionally, ring-core fiber designs for orbital angular momentum modes transmission have been considered for reduced crosstalk due to their helical phase front, as modes remain orthogonal to each other [20-24].

Elliptical core multimode fibers (EC-MMF) have gained attention for SDM transmission due to their reduced modal coupling, which simplifies DSP for coherent data transmission and enables SDM for datacenters at a lower power consumption [25-28]. The asymmetry in refractive index profile with respect to fiber axis of EC-MMF results in different propagation constants for the linearly polarized modes in each mode group, thereby reducing intra-mode coupling. Since the intra-mode group crosstalk is reduced in the fiber, intra-mode group crosstalk in the transmission link is primarily influenced by mode multiplexers (MUX) and mode demultiplexers (DMUX), at least for short distances ~1 km [26]. The profile asymmetry of the fiber results in the support

Submitted to IEEE/Optica Journal of Lightwave Technology on 2025 xxx xx, this work was supported by the UKRI Future Leaders Fellowship [MR/T041218/1] and [MR/Y034260/1]; Engineering and Physical Sciences Research Council (EPSRC) Doctoral Studentship Grant reference [EP/R513143/1] and [EP/W524335/1]. (Corresponding author: Rekha Yadav).

Rekha Yadav, Fabio A. Barbosa and Filipe M. Ferreira are with the Optical Networks Group, Department of Electronic and Electrical Engineering, University College London (UCL), London WC1E7JE, UK. (e-mail: rekha.yadav.22@ucl.ac.uk, fabio.barbosa@ucl.ac.uk, f.ferreira@ucl.ac.uk).

Ming-Jun Li is with the Science and Technology Division, Corning Incorporated, Corning, NY 14831 (email: lim@corning.com). Color versions of one or more figures in this article are available at https://doi.org/xxxx. Digital Object Identifier xxxx.

of hybrid modes, and while Ince-Gaussian (*IG*) modes have been proposed for EC-MMF, the performance in terms of crosstalk for Hermite-Gaussian (*HG*) and *IG* modes remains equivalent [29]. Consequently, modes in EC-MMF can be approximated well by Hermite-Gaussian modes, that can be divided into even and odd modes with distinct lobes and phase patterns in the transverse direction. Conveniently, *HG* modes have been shown to be compatible with advanced programmable mode multiplexers based on multi-plane light conversion (MPLCs), which have been shown to scale for a large number of modes [30-32]. EC-MMF along with MPLCs can be used to reduce the intra-mode group crosstalk in the link for short distances. Further, EC-MMF can be made using a conventional fiber manufacturing process [26]. A thorough study of the impact of core ovality on the signal transmission is important for both deliberately elliptical core fibers and fibers with core-ovality imperfections due to refractive-index fluctuations caused during manufacturing [33].

Previous studies on elliptical core fiber transmission have focused on "few-mode fibers" over a short range of distances (0.5 km to 1 km), supporting a few linearly polarized (*LP*) modes [34-36]. Mode group delay has also been shown to decrease with the ovality for the EC-MMF [37]. Recently, we have shown that the EC-MMF also reduces intra-mode group crosstalk, reducing overall complexity [38]. In this manuscript, we extend the previous studies by providing a discussion on the physics behind the reduction in intra-mode group crosstalk and mode group delay. We quantify the effect of ovality on modal analysis and modal delay, ranging from 0.1 % to 40 % for the fiber supporting different number of modes up to 90-polarization modes, and find the optimum ovality values to have minimum intra-mode group crosstalk. We also investigate data transmission over 10 km fiber links with coherent detection, comparing the performance of elliptical and circular fibers. Reducing intra-mode group crosstalk allows MIMO-free transmission in fibers with minimal inter-mode crosstalk. However, crosstalk is non-homogeneous, with adjacent mode groups exhibiting finite crosstalk even in the weak-to-intermediate coupling regime. We show that using the worst-mode interferers as an input to the equalizer can have better performance rather than using the MIMO of mode group size for each mode with the same complexity as in a standard MGDM scenario [15], when all the modes are excited in the fiber. Further, we show using elliptical-core fibers with worst-mode interferers equalization scheme reduces the complexity-compared to circular-core fibers. We find the modes having minimum number of interferers to recover a 99 % signal power from the channel crosstalk matrix, and purpose to use these modes for the transmission when transmitting data in less tributaries than the maximum, and this helps in achieving a large throughput at the less complexity.

The manuscript is organized as follows. Section II discusses the refractive index profile and guiding properties of elliptical core MMF, focusing on the impact of fiber asymmetry on mode behavior. Section III discusses the effect of ovality on the modal characteristics and identifies the optimal ovality to have minimal intra-mode group crosstalk. Section IV presents the simulation results for the transmission of polarization mode multiplexed 16-QAM signals transmitted over the elliptical core fiber, quantifying the performance in terms of signal-to-noise ratio, equalization complexity and throughput. Conclusions are drawn in Section V. Note that mode counting refers to polarization modes unless specified; for example, fiber supporting LP_{01} and LP_{11} correspond to six polarization modes (three spatial modes and two linearly polarized modes).

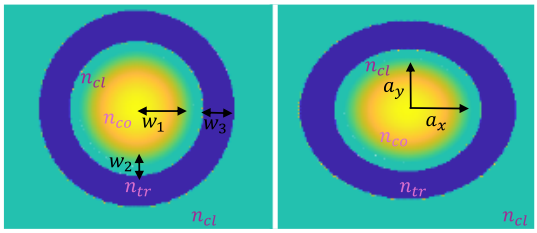

Fig. 1. Fiber refractive index profile distribution along with geometry for (a) Circular core fibers, and (b) Elliptical core fibers.

II. FIBER PROFILE DESCRIPTION AND ANALYSIS

The refractive-index profile for circular core fibers consisting of a graded index core and a cladding trench is initially optimized to reduce modal delay and maximize the information throughput for a given fiber, following the same procedure as in [13]. Fig. 1 (a) presents a schematic of a circular core profile, where n_{co}, n_{tr} and n_{cl} represents the refractive index of core, trench and cladding respectively. The core radius (w_1) is 23.51 µm, core to trench distance (w_2) is 1.25 µm and trench width(w_3) is 5 µm for 90-polarization mode circular fibers with a core-clad contrast of 0.01. w_1 increases with the supported number of modes [13]. Ovality in the fibers is defined as,

$$\chi = \frac{2(a_x - a_y)}{a_x + a_y} \tag{1}$$

where a_x and a_y represents the semi-major and semi-minor core radii respectively. Here, ovality is introduced in the optimized fibers by rescaling the grid spacing of the axis such that, x-axis is scaled by a factor of $\xi = \sqrt{(1+\chi/2)/(1-\chi/2)}$ and y-axis by a factor of $1/\xi$, keeping the core area and graded exponent (α) same as circular fiber. This makes the core asymmetric and alters the refractive index along both axes as shown in Fig. 1 (b). The refractive index profile as a function of x-axis coordinate ρ_x and y-axis coordinate ρ_y for elliptical fibers is described below, assuming z-axis and fiber axis coincide [39]:

$$n(\rho_x,\rho_y) = \begin{cases} n(0)\sqrt{1-2\Delta n_{co}\left\{\left(\frac{\rho_x}{a_x}\right)^2+\left(\frac{\rho_y}{a_y}\right)^2\right\}^{\alpha/2}}, & \left\{\left(\frac{\rho_x}{a_x}\right)^2+\left(\frac{\rho_y}{a_y}\right)^2\right\}<1 \\ n_{cl}, & \left\{\left(\frac{\rho_x}{a_x}\right)^2+\left(\frac{\rho_y}{a_y}\right)^2\right\}\geq 1>\left\{\left(\frac{\rho_x}{b_x}\right)^2+\left(\frac{\rho_y}{b_y}\right)^2\right\} \\ n_{cl}/\sqrt{1-2\Delta n_{tr}}, & \left\{\left(\frac{\rho_x}{b_x}\right)^2+\left(\frac{\rho_y}{b_y}\right)^2\right\}\geq 1>\left\{\left(\frac{\rho_x}{c_x}\right)^2+\left(\frac{\rho_y}{c_y}\right)^2\right\} \\ n_{cl}, & \left\{\left(\frac{\rho_x}{c_x}\right)^2+\left(\frac{\rho_y}{c_y}\right)^2\right\}\geq 1 \end{cases} \tag{2}$$

Here, $n(0)$ is the refractive index of the core at center, $b_x = \xi.(w_1+w_2)$, $c_x = \xi.(w_1+w_2+w_3)$, $b_y = b_x/\xi^2$ and $c_y = c_x/\xi^2$. Δn_{co}

This article has been accepted for publication in Journal of Lightwave Technology. This is the author's version which has not been fully edited and content may change prior to final publication. Citation information: DOI 10.1109/JLT.2025.3603881

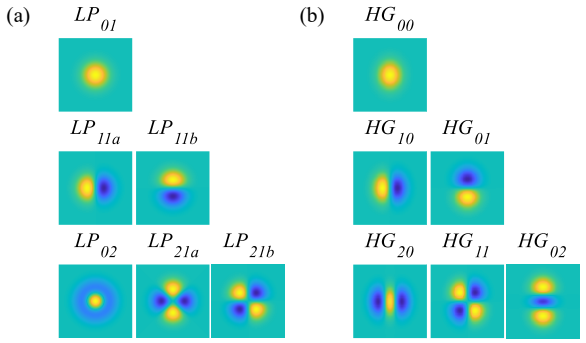

Fig. 2. Spatial electric field distribution for a 6-spatial mode fiber with a core-clad contrast of 0.01, (a) Circular core fibers, and (b) Elliptical core fibers with an ovality of 11.7 %.

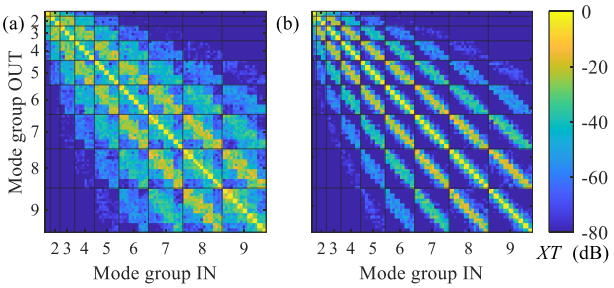

Fig. 3. Power coupling between modes (a) Circular (0 % ovality), (b) 11.7 % ovality for a fiber with 90 polarization modes, 10 km long, crosstalk strength as -20 dB/km, and core-cladding contrast = 0.01. Black lines represent the mode group boundaries.

and Δn_{tr} are the relative refractive index difference at the core and trench respectively.

The asymmetry in the refractive index profile directly impacts the spatial distribution of the electric and magnetic fields, affecting the fiber guiding properties [40, 41]. Fig. 2 shows the electric field distribution of the 6-spatial mode fiber with a core-clad contrast of 1 % for the circular and elliptical core fiber with an ovality of 11.7 %. In circular core fibers, modes are described using cylindrical coordinates where field lines are perfectly axially symmetric in the core, allowing the modes to be classified into transverse electric, transverse magnetic, and hybrid *EH* and *HE* modes [42]. However, in elliptical core fibers the asymmetry disrupts the separability of electric and magnetic fields resulting in the support of only hybrid modes [41]. These modes are better approximated by *HG* modes as shown in Fig. 2 (b), unlike the standard *LP* modes used for circular fibers under weakly-guiding approximation [29, 34]. The impact of ovality-induced non-uniformities on mode confinement and overall mode profile varies between odd and even *LP* modes due to their different symmetrical properties as can be seen from Fig. 2 (b) for LP_{21a} and LP_{21b} modes respectively. The differing boundary conditions and mode confinement along the major and minor axes result in modes polarized along these axes to experience different effective indices compared to the circular core fibers [41]. This results in distinct mode propagation constants, breaking the degeneracy of the *LP* modes typically observed in circular core fibers. Here, a vector finite difference mode solver is used to find mode solution of the fiber employing a grid step size of 0.2 µm and grid size of 4-times the total radius (c_y) [43]. The algorithm iteratively find the roots of the characteristic equation, and recalculates them as the ovality changes.

Multimode fibers support multiple spatial modes, and due to perturbation in the refractive index of a fiber arising from manufacturing variations, or stress; these spatial modes exchange power between them, leading to the modal coupling during transmission. Typically, the fiber mode coupling strength for a spatial mode m is defined as $XT_m = \sum_{v \neq m} P_v / P_m$, where P_v is the power coupled into an interfering spatial mode v, and P_m, is the remaining power in the launched spatial mode m after propagation over a certain distance. This definition is used to set the fiber crosstalk strength throughout the manuscript. Note that each spatial mode m accounts for power in both the polarization states. In MMFs, spatial modes are grouped into mode groups, such that any LP_{mn} mode belongs to the mode group indexed by m+2n-1, where m and n denotes the azimuthal and radial nodes of the mode respectively. To understand the impact of ovality on the coupling within the mode group, we define intra-mode group crosstalk for a spatial mode m, which is given as $Intra\text{-}XT_m = 1 / (M_i - 1) \sum_{v \in i, v \neq m} P_v / P_m$, where M_i is the total number of spatial modes in mode group i ($M_i - 1$, to exclude the launched spatial mode m), and P_v is the power in the interfering spatial mode v within the same mode group i, and P_m is the power in the launched spatial mode m after propagation. Similarly, the inter-mode group crosstalk strength from an input spatial mode LP_{mn} to an output mode LP_{kl}, where the output mode belongs to the different mode group than the input mode, is defined as, $Inter - XT_{LP_{mn} \to LP_{kl}} = \frac{\sum_{u+2v=k+2l} P_{(mn)\to(uv)}}{(k+2l-1) \sum_{p+2q=m+2n} P_{(mn)\to(pq)}}$, where the numerator represents the total power coupled from the input mode LP_{mn} into all spatial modes within the target mode group $k + 2l - 1$, and the denominator normalizes this with respect to the number of modes in the output mode group and the total coupled power within the input mode group m+2n-1, this definition neglects the intra-mode group interactions and accounts for the varying number of modes in different mode group.

Fig. 3 shows the power coupling matrix for a 90-polarization mode fiber with a core-cladding contrast of 0.01 for a 10 km length with section length (dz) = 1 m, and crosstalk strength of the fiber as - 20 dB/km, (a) circular (0 % ovality) fiber, (b) 11.7 % ovality. The crosstalk strength depends on the combination of ovality and longitudinal perturbations (radial displacement between sections). The radial displacement sets the inter-mode group crosstalk strength, which is dominated in the fiber link. Therefore, when the ovality changes, one can maintain the same average crosstalk strength by changing the radial displacement accordingly. In Fig. 3 (a), it can be observed that certain modes within the mode group of the launched mode have lower power than the modes in the adjacent mode group. This highlights the non-uniform nature of fiber crosstalk in the circular fibers, where power coupling is influenced by both mode overlap and the difference in propagation constants between modes. In some cases, a given mode may have a higher mode overlap with the modes in the adjacent mode group than with certain modes within its own mode group, resulting in higher coupling from the adjacent mode group. From Fig. 3 (b), it has been observed that the

This article has been accepted for publication in Journal of Lightwave Technology. This is the author's version which has not been fully edited and content may change prior to final publication. Citation information: DOI 10.1109/JLT.2025.3603881

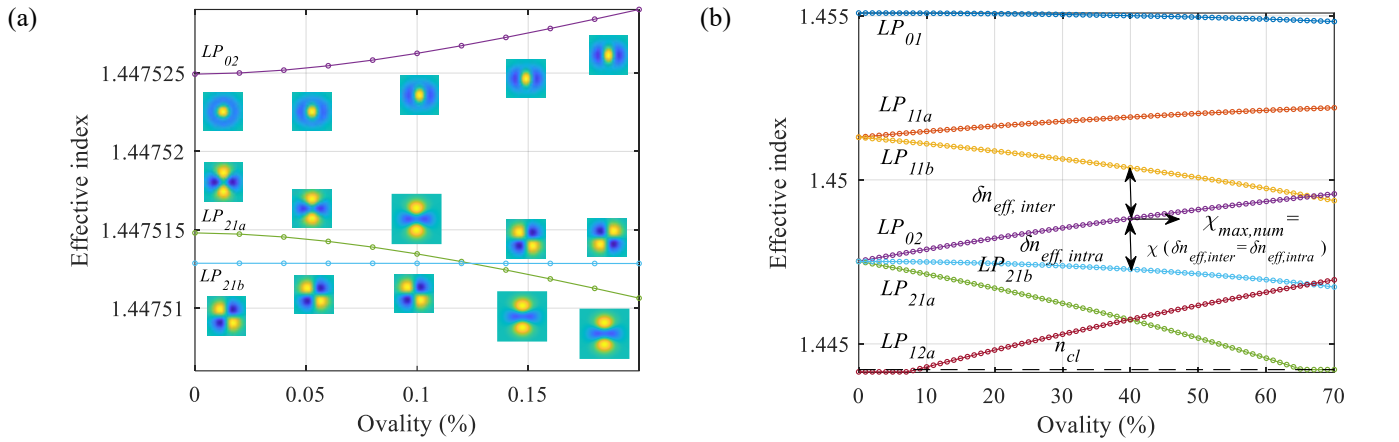

Fig. 4. Effective index for X-polarization as a function of the ovality for the fiber with 12-polarization modes, and a core-cladding contrast of 0.01, (a) Last mode group of the fiber for a small ovality values, (b) All guided modes of the fiber including one radiation mode for a large range of ovality values, dashed (- -) line represents the cladding index of the fiber.

coupling between the modes within the mode group reduces with core-ovality.

III. EFFECT OF OVALITY ON FIBER CHARACTERISTICS

A. Variation of effective index with ovality

Fiber core design significantly influences the effective index (n_{eff}) of the modes. Fig. 4 (a) shows the variation of the effective index computed using mode solver (vectorial solution) for the X-polarization for a very small range of ovality values, for the last (3rd) guided mode-group of a fiber supporting 12-polarization modes with a core-cladding contrast of 0.01. For circular fiber, the effective index difference between the degenerate modes (LP_{21a} and LP_{21b}) is small, about an order of magnitude lower than the difference between the effective indices of LP_{02} and LP_{21a}. This results in stronger coupling between the degenerate modes compared to a pair of non-degenerate modes. When ovality is introduced, the effective indices of modes start to change due to variations in the refractive index profile along the major and minor axis. For very small ovality values (below 0.12 %), difference in effective indices between degenerate modes decreases, increasing their coupling. These ovality values can arise randomly during manufacturing process. Although the variation in n_{eff} appears only at the fourth decimal place, such small differences can still produce a significant physical impact in high-performance fiber systems. These deviations can influence the group velocities of modes and intra-mode group coupling. While inter-mode group characteristics remain largely unaffected due to sufficient mode separation, the intra-mode group behavior, particularly coupling between degenerate modes, can become sensitive, potentially resulting in modal dispersion or increased crosstalk, particularly in mode-division multiplexing systems where modes within a mode group are treated independently.

With further increase in ovality, the effective indices difference between adjacent modes of the mode group increase, breaking the degeneracy of the modes. Modes confined along the semi-major axis experience larger variation in core index than those along the semi-minor axis, leading to an increase in the effective index for the modes majorly confined along the major axis. Whereas there is a decrease in the effective index for the modes confined along the minor axes. Here, the effective index of LP_{21b} does not change as the power (modal confinement) is equally distributed along both azimuthal fiber core axis as shown in Fig. 2 (a). With ovality, its modal distribution remains the same as HG_{02} in Fig. 2 (b), whereas the maximum modal power in LP_{02} and LP_{21a} is confined along one of the major and their effective indices changes depending on their modal confinement along the major and minor axes respectively.

Fig. 4 (b) shows the effective indices of X-polarization for all guided modes and one radiation mode (LP_{12a}) of the 12-polarization mode fiber over a large range of ovality values. Since LP_{01} is equally confined with respect to both fiber axes, its effective index remains nearly unchanged with increasing ovality. In contrast, LP_{11a} modal power is confined along the major axis; thus, as the major radius increases with the ovality, its effective index also increases. Similarly, LP_{11b} effective index decreases as the minor radius of the fiber decreases with ovality. The average effective index difference between the adjacent modes within the same mode group is referred to as $\delta n_{eff,intra}$. As ovality increases, the effective indices of the mode's changes, leading to an increase in $\delta n_{eff,intra}$. The increase in the effective index difference within the mode-group reduces the coupling between modes within the mode group, until it affects the modes in the adjacent mode group. In weakly guiding circular fibers, modes are grouped based on similar propagation constants [18]. The effective index spacing between adjacent mode groups decreases with increasing group order. As a result, the smallest effective index difference among all adjacent mode groups typically occurs between the penultimate and final mode groups. Therefore, from a design perspective and neglecting the effect of mode overlap (since significant coupling requires both mode overlap and phase matching), the upper limit for the optimum ovality is determined by the difference in effective index between the last mode in the penultimate mode group and the first mode in the last mode group. When this inter-group effective index difference ($\delta n_{eff,inter}$) becomes equal to the average intra-group effective index difference of the adjacent modes within the last mode group, the ovality is considered to reach its maximum limit. The numerically calculated maximum ovality

This article has been accepted for publication in Journal of Lightwave Technology. This is the author's version which has not been fully edited and content may change prior to final publication. Citation information: DOI 10.1109/JLT.2025.3603881

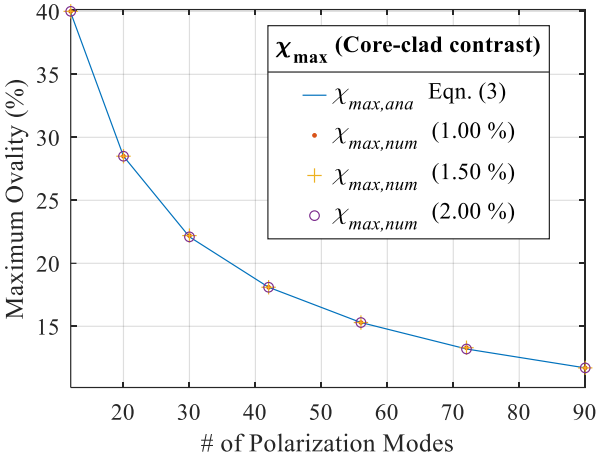

Fig. 5. Maximum ovality as a function of the supported polarization modes in fiber for the different core-clad contrast values.

values ($\chi_{max,num}$) for the fibers supporting different number of polarization modes are presented in Fig. 5 for different core-clad contrasts using markers. With an increase in the core-clad contrast values, the difference between the effective indices of modes from adjacent mode groups increases in circular fibers. This results in a corresponding increase in $\delta n_{eff,intra}$ and $\delta n_{eff,inter}$, while the maximum ovality remains unchanged. Further, we propose a method to derive analytically maximum ovality ($\chi_{max,ana}$) values based on the based on the effective indices derived using the scalar field theory, as discussed in Appendix I. On solving Eqn (13) of Appendix I, maximum ovality value analytically is given as,

$$\chi_{max,ana} = \frac{2}{2N_{mg} - 1}, \tag{3}$$

which is independent of core dimensions. Although there is a discrepancy in the criteria used to obtain maximum ovality value between analytical ($\chi_{max,ana}$) and numerical method ($\chi_{max,num}$), we observe that the computed maximum ovality values analytically coincide with the above numerical values as shown in Fig. 5.

Moreover, as observed in Fig. 4 (b), beyond an ovality of 9 %, LP_{12a} mode (the radiation mode for circular fibers) is guiding in the fiber, though the effective index is close to the cladding index for ovalities less than the identified maximum limit. But beyond an ovality of 40 % (maximum ovality as shown in Fig. 5 for 12-mode fiber), LP_{21a} mode propagates with a lower effective index than LP_{12a}, altering the mode distribution for the guided modes and increasing the coupling between the modes in the last mode group. Though ovality increases the number of guided modes, we consider only the modes propagating with the highest effective indices in this manuscript, to ensure that the set of modes analyzed remains comparable to those in circular fibers and modes propagating with effective indices closer to cladding index will get lost with bending losses in the transmission.

Fiber birefringence also changes with ovality, and the difference in effective index between polarizations of respective modes also increases with ovality. However, the difference between effective index of polarization modes is less than 10^{-5} for multimode fibers even for higher ovality values. Therefore, coupling between the polarization modes would still be maximum. And, with the use of stress rods, these fibers can be designed to polarize maintaining fibers with low coupling between polarization modes [44]. Also, the difference between effective indices of two polarizations decreases for a given ovality with the growing number of modes supported in the fiber.

B. Effect of ovality on intra-mode group crosstalk strength with random perturbation: single fiber section

To analyze the effect of modal coupling in fibers due to the perturbations arising in the manufacturing process, we consider a single section of fiber with step length (*dz*) of 1 m. Fig. 6 shows the average intra-mode group coupling strength over the modes by varying the normalized radial displacement (radial displacement with respect to core radius). Each data point averages over 10,000 combinations of azimuthal and polarization rotation values for a 90-polarization mode fiber having a core-cladding contrast of 0.01. The fiber transfer matrix is defined by propagation constants, modal coupling and polarization rotation, calculated following a method described in [45]. As expected, the average intra-mode group *XT* increases with the radial displacement for circular fibers, as the increase in mode overlaps leads to more coupling between the modes. This trend remains similar for the elliptical core fibers, but with increasing ovality, intra-mode group *XT* initially decreases and stabilizes to a minimum value up to 11.7 %, beyond which it again increases. Please note here, 11.7 % ovality is the maximum ovality limit for a 90-polarization mode fiber as shown in Fig. 5. The suppression in intra-mode group *XT* decreases from 40 dB to 25 dB with the increase in the normalized radial displacement from 10^{-3} to 0.02. Further, the radiant mode (previously for a circular fiber) guides with an effective index larger than one of the guided modes (for the circular fiber) beyond the maximum ovality limit as seen from Fig. 4 (b). Due to the change in modal profile of the modes beyond the maximum ovality limit, the slope of the intra-mode group crosstalk changes with respect to the radial displacement. Also, this changes the mode overlap for the last considered mode group, directly increasing the intra-mode group crosstalk. Further, the inter-mode group strength has a negligible effect of ovality, up to the identified maximum ovality value (11.7 %), as the difference between

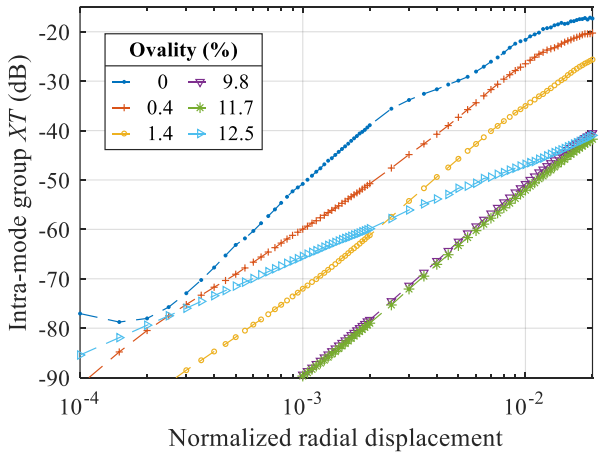

Fig. 6. Averaged intra-mode group *XT* over modes as a function of the normalized radial displacement for a fiber with 90-polarization modes, and a core-cladding contrast of 0.01. Results averaged over 10.000 azimuthal displacement and polarization rotations.

This article has been accepted for publication in Journal of Lightwave Technology. This is the author's version which has not been fully edited and content may change prior to final publication. Citation information: DOI 10.1109/JLT.2025.3603881

effective indices between modes of adjacent mode groups remains larger than the $\delta n_{eff,intra}$.

C. *Effect of ovality on intramode group crosstalk strength: multi fiber section*

In this section, we extend the study of intra-mode group *XT* to multi-fiber sections. We analyze a fiber with a length (L) of 10 km, dz = 1 m, and a core-clad contrast of 0.01. The crosstalk strength in the fiber is set using the radial displacement, determined from the single-section analysis by varying the normalized radial displacement. This analysis averages over 10,000 points of azimuthal displacement and polarization rotations for a given ovality. Based on this, we calculate the required radial displacement required per section to maintain a fixed crosstalk strength across fibers with different ovality values. In the multi-section model, each section introduces a random azimuthal displacement and polarization rotation, following the method described in [45], while assuming that refractive index remains constant over the section length. This assumption holds as long as the section length is shorter than the correlation length of the actual imperfections [10], which is typically the case for imperfections in fiber. The variation in the required radial displacement with ovality ensures the consistency of the crosstalk strength. The accumulated transfer matrix for a multi-section fiber is obtained by multiplying the transfer matrices of each individual section. Fig. 7 (a) shows the average intra-mode group *XT* over the mode groups as a function of ovality values. We observe that the intra-mode group *XT* behavior for very low ovality values (up to 0.12 %), depends on the number of modes supported by fiber. For some modes, *XT* increases slightly, while for others it decreases or remains relatively constant before it starts decreasing. This indicates a non-monotonic and mode-dependent response in this region, because fibers are initially optimized for low differential mode delay as shown in [13], before introducing ovality. Further increasing ovality leads to a decrease in the intra-mode group *XT* to a minimum value as the difference of the effective indices between the degenerate modes increases. Beyond 1 % ovality, the fiber supporting different number of modes tend to reach a near minimum in intra-mode group *XT* values as observed in Fig. 7 (a). However, in Fig. 6, the intra-mode group *XT* continues to decrease up to an ovality of approximately 9.8 %. This is due to the presence of inter-mode group *XT* in the multi-section link. Since, mode coupling is considered across all mode pairs in each section and measurements are performed at the end of transmission. Although the specific source of the coupling can no longer be identified at that point, the measurement reflects the cumulative effect of propagation. Since there are more modes outside a given mode group than within it, the measured accumulated intra-mode *XT* (which may be reduced by ovality) cannot be smaller than the contribution imposed by coupling interactions with all other modes outside the respective group. As a result, the observed plateau in intra-mode group *XT* maximum suppression is determined by the inter-mode group crosstalk present in the multi-section link, which is absent in single-section case of Fig. 6. Also, the maximum suppression with optimized ovality compared to circular fibers decreases for the 10 km link, compared to the single section, the plateau is decided by the inter-mode crosstalk, which gets accumulated in the multi-section link. Further, intra-mode group *XT* remains at a minimum level for a range of ovality values and beyond this range, increasing ovality substantially increases intra-mode group *XT*. This trend is also seen in the intra-mode group *XT* characteristics shown in Fig. 6 for an ovality of 12.5 %. Fig. 7 (a) also highlights the identified maximum ovality values ($\chi_{max,ana}$, which also equals to $\chi_{max,num}$) in section III-A, and it can be observed that beyond these values, crosstalk increases substantially (more than 5 dB for a relative small increase in ovality values over a log scale) for fibers supporting modes between 12 and 90. The substantial increase in the intra-mode group crosstalk is due to the fact that, beyond the maximum ovality value, the radiant mode in the elliptical core fibers begins to guide with an effective index higher than that of a guided mode in the circular fiber, as shown for 12-polarization mode fiber in Fig. 4 (b). This alters the mode overlap in the last mode group (highest effective indices modes are considered for analysis) as discussed in section III-B for an ovality of 12.5 %. This is the same reason as for smaller number of modes, that's when adjacent mode groups cross as shown in Fig. 4 (b) for 12-mode fiber. The maximum intra-mode group crosstalk suppression is calculated as the difference between maximum and minimum intra-mode group crosstalk values within the range of ovality from 0 to 11 % (maximum ovality value from where the *XT* starts increasing substantially). For fiber supporting 90-polarization modes, the

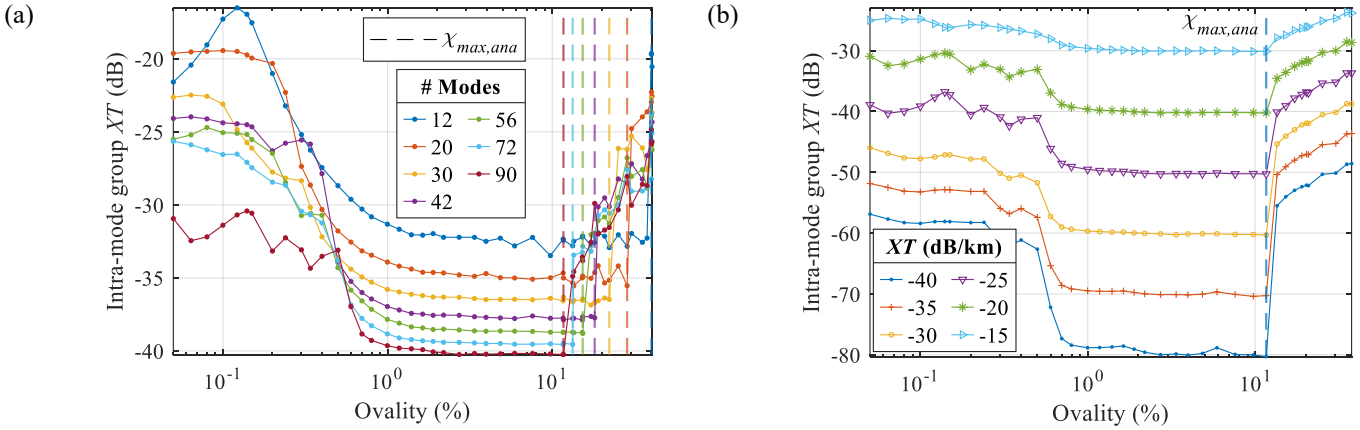

Fig. 7. Intra-mode group *XT* averaged over modes by varying ovality for 10 km long fiber, (a) for different number of polarization modes in the fiber with crosstalk strength of – 20 dB/km, (b) for different fiber crosstalk strength set by radial displacement in a 90-polarization mode fiber. Results averaged over 500 times by varying the azimuthal displacement and polarization rotation for each fiber section.

This article has been accepted for publication in Journal of Lightwave Technology. This is the author's version which has not been fully edited and content may change prior to final publication. Citation information: DOI 10.1109/JLT.2025.3603881

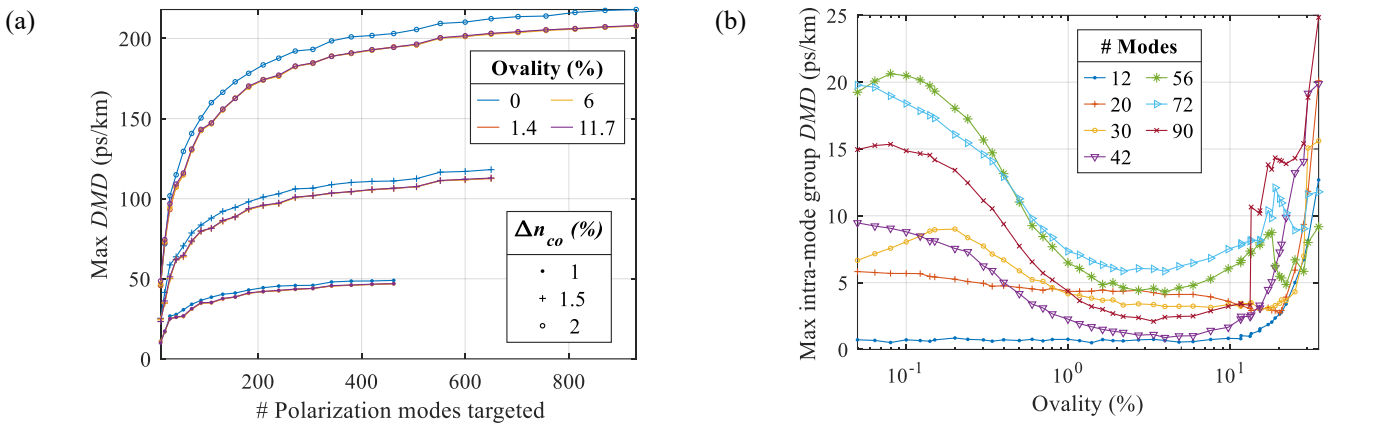

Fig. 8. (a) Maximum differential mode delay (*DMD*) as a function of the number of polarization modes targeted in a fiber, considering different core-cladding index differences and a range of ovality values. (b) Maximum of intra-mode group *DMD* calculated over mode group as a function of fiber core ovality for fibers supporting varying numbers of polarization modes.

maximum suppression is approximately 11 dB, and it increases with the decrease in the number of modes supported by fiber. Further, it can be observed that the intra-mode group *XT* values for circular fibers don't follow any trend with the number of modes supported in the fiber as they are optimized for low *DMD,* while there is a decrease in the maximum intra-mode group crosstalk suppression value possible for the optimized ovality range with the increase in supported modes.

Fig. 7 (b) shows the intra-mode group *XT* by varying ovality values for a 90-polarization mode fiber across different fiber crosstalk strength values, which are set by the radial displacement required per section. As the fiber crosstalk strength increases, the maximum reduction possible with optimized ovality in intra-mode group crosstalk level also decreases, as inter-mode group crosstalk strength increases linearly in the fiber. However, the range of optimized ovality values to have minimize intra-mode group crosstalk remain consistent regardless of the fiber coupling strength.

D. Impact on DMD variation with ovality

Fibers are initially optimized to have a low differential mode delay for the circular cores, ensuring the maximum throughput. Ovality is then introduced into optimized fibers, impacting the effective indices of modes and, their group velocities. Fig. 8 (a) illustrates the variation of maximum *DMD* with increasing ovality across fibers supporting a different number of polarization modes. The maximum *DMD* corresponds to the highest *DMD* among all mode pairs over the C-band, excluding the modes in the last mode group due to higher bending losses and unsuitability for data transmission [13]. For a given core-clad contrast, *DMD* increases rapidly with the number of modes and then saturates for circular fibers. Interestingly, ovality has a nearly negligible impact on the maximum *DMD* compared to circular fibers. This is because *DMD* is calculated from the group effective index of the mode, which is given by,

$$n_{g,LP_{mn}} = n_{eff,LP_{mn}}(\omega) + \omega \frac{\delta n_{eff,LP_{mn}}}{\delta \omega}, \quad (4)$$

where ω is the angular frequency of the wave. With increased ovality, modes with more power along the minor axis have weaker confinement and larger wavelength dependence, while modes along the major axis exhibit the opposite trend. Due to the opposite effect of ovality on effective index and its wavelength dependence for a given mode, results in an overall *DMD* to remain approximately the same. Moreover, as expected *DMD* scales with the core-clad contrast due to the increase in $\delta n_{eff,inter}$.

Fig. 8 (b) shows the variation of maximum of intra-mode group *DMD*, which is the worst intra-mode group *DMD* over all the mode groups excluding the last mode group, with ovality for a fiber supporting different number of spatial modes with a core-clad contrast of 1 %. The intra-mode group *DMD* is calculated as the worst *DMD* among pairs of modes within the same mode group. The maximum of intra-mode group *DMD* shows different behavior than the overall *DMD* shown in Fig. 8 (a). In circular fibers, the intra-mode group *DMD* increases with the order of mode groups as the higher mode groups are closer to the cladding index and therefore have larger wavelength dependence. However, with EC-MMF optimized for ovality, the intra-mode group *DMD* becomes uniform across mode groups. This is because, for the modes along the major axis, effective index increases with ovality have a lower wavelength dependence due to being more confined towards the core, and vice versa for the modes along the minor axis. Consequently, the difference in group effective index within the mode group decreases with increasing ovality, an effect more prominent in higher mode groups. This results in a decrease in the intra-mode group *DMD* with ovality. Intra-mode group *DMD* decreases with increasing ovality up to a sub-optimal point, after which it starts increasing. For 90-polarization mode fiber, a reduction in maximum intra-mode group *DMD* by approximately 6*x* times is observed for optimized ovality compared to the circular fibers. The minimum intra-mode group *DMD* is observed at an ovality of 3 % of 2.11 ps/km, with approximately a stable performance from an ovality of 1.5 % to 8 % for a 90-polarization mode fiber. This is the lowest *DMD* reported so far in for multimode fibers [26, 36]. Also, the maximum intra-group *DMD* for circular fibers doesn't follow any trend with the number of modes supported, with the maximum reduction observed for a 42-polarization mode fiber due to initial optimization for overall *DMD*.

E. Impact on mode dependent loss with ovality

In practical fiber systems, spatial modes experience different mode dependent loss (*MDL*) due to Rayleigh scattering,

This article has been accepted for publication in Journal of Lightwave Technology. This is the author's version which has not been fully edited and content may change prior to final publication. Citation information: DOI 10.1109/JLT.2025.3603881

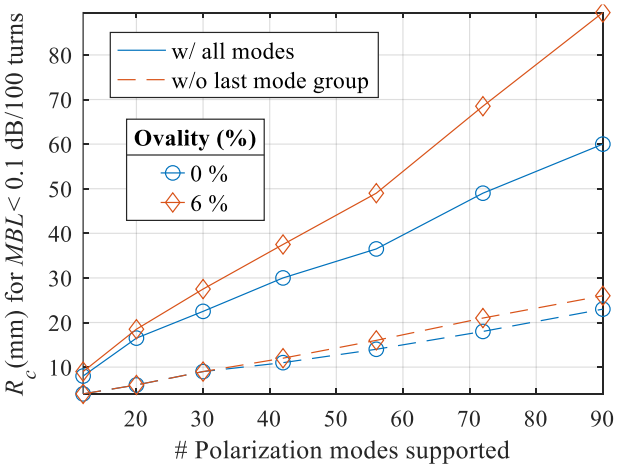

Fig. 9 (a). Minimum bending radius to have *MBL* for the modes considered below 0.1 dB for 100 turns, for the circular and elliptical core fibers with a core-clad contrast of 0.01 %. 'Line' represents R_c while considering *MBL* over all modes and 'Dashed lines' by considering *MBL* of all modes except the modes in the last mode group.

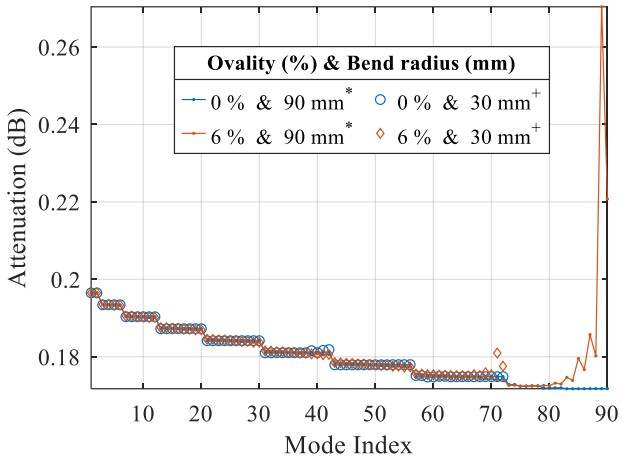

Fig. 9 (b). Attenuation (dB) for a 90-polarization mode fiber with a core-clad contrast of 0.01 %, which is sum of losses from Rayleigh scattering for 1 km, confinement loss for 1 km, and bending loss induced by 100 turns. Results are shown for a bending radius of 90 mm including all mode groups (* -), and for a 30 mm bend radius excluding the last mode group (+-).

confinement loss, and macro-bending. To analyze the effect from each of them, we first calculate macro-bending loss (*MBL*) for a core-clad contrast of 0.01 % using a conformal mapping technique that incorporates bending into the fiber refractive index profile [46]. To extend the analysis to smaller bend radii, a perfectly matched layer was added at the caustic radius as described in [47]. Complex eigenmodes of the bent fiber were solved, and *MBL* was calculated from the imaginary part of the effective indices. To account for orientation dependent bending effects, *MBL* was computed over bending angles from 0 to 180° relative to the fiber's X-axis, and mean *MBL* was used for each mode at a given bend radius. Fig. 9 (a) shows the minimum bending radius (R_c) required to ensure that the maximum *MBL* across all modes is below 0.1 dB for 100 turns. As expected, R_c increases with the number of modes supported in the fiber, for both circular and elliptical core fibers. Notably, for a 90-mode elliptical core fibers, R_c is about 30 mm larger than that of a circular fibers when all the modes are considered. However, this increase is primarily driven by the last mode group. When the last mode group is excluded, the bending radius requirement is significantly relaxed, for example, at 90 modes, the difference in R_c between circular and elliptical fibers is reduced to only ~1 mm.

Further, we calculated the mode-dependent attenuation due to Rayleigh scattering using the method described in [48], which shows that that lower-order modes experience higher loss due to stronger field intensity in the core where Rayleigh scattering is most pronounced. And, the confinement loss was calculated using the method described in [49], and it increases with the mode-group order, as higher-order modes are weakly confined to the core and more susceptible to leakage. Fig. 9 (b) shows the total attenuation per mode for a 90-polarization mode fiber with a core-clad contrast of 0.01 %, accounting for Rayleigh scattering loss and confinement loss over 1 km fiber length, and *MBL* for 100 turns. Two scenarios are considered: (a) all modes considered at a bending radius of 90 mm (this is chosen because as shown in Fig. 9 (a), required R_c for elliptical-core fibers) , and (b) all modes except the last mode group with a bending radius of 30 mm (this is chosen as it's a standard bending radius for single-mode fibers). Fig. 9 (b) shows that excluding the last mode group significantly reduces modal loss variation, and the standard deviation of uncoupled modal attenuation becomes comparable between circular and elliptical core fibers.

IV. Effect of Ovality on Modulated Signal Transmission

In this section, we quantify the effect of ovality on the performance of 32 GBd 16-QAM modulated signal SDM transmission as shown in Fig. 10, assuming an ideal transmitter. The modulated signal is then transmitted over a 90-polarization mode fiber with core-clad contrast of 0.01, length 10 km having an attenuation of 0.2 dB/km, and a fiber crosstalk strength of - 20 dB/km. The differential group delay between the polarizations is assumed as 1 fs. The transmitted signal experiences an average modal dispersion of 21 ps/nm.km, modal coupling, and polarization rotation at each step along the fiber, with a step length of 1 m, as described in section III-C. The amplified spontaneous emission (ASE)

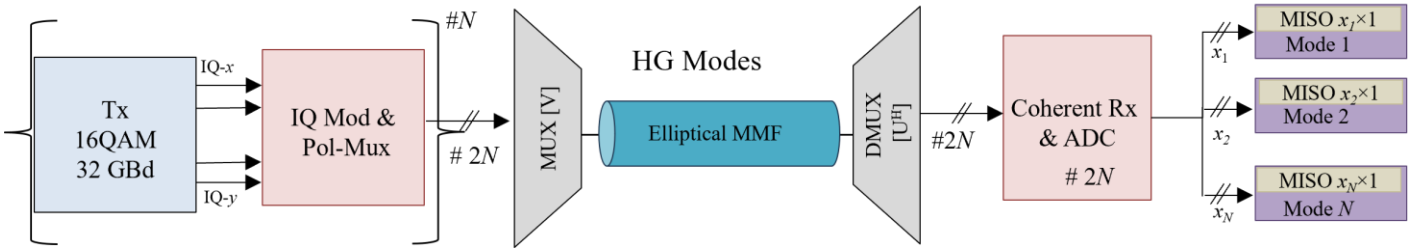

Fig. 10. Simulation setup for data transmission over *M*-modes EC-MMF, and DSP equalization considered at the receiver. Tx and Rx represents transmitter and receiver respectively, DP-IQ Mod represents dual polarization in-phase and quadrature modulator.

This article has been accepted for publication in Journal of Lightwave Technology. This is the author's version which has not been fully edited and content may change prior to final publication. Citation information: DOI 10.1109/JLT.2025.3603881

noise is then added to the amplified signal such that the optical signal-to-noise-ratio (*OSNR*) in the reference bandwidth of 12.5 GHz is set to 35 dB for all the launched signals in the fiber. The signal in all the transmitted modes is then detected by employing a polarization diverse coherent receiver for each tributary. The received signal undergoes post-processing using the multiple-input-single-output (MISO) equalizer to counteract the channel effects. The symbol-rate sampled input MISO equalizers are implemented in the frequency domain with a 4096-point fast Fourier transform (FFT), and the equalizer coefficients are calculated using the least squares criterion, assuming the full channel estimation available at the receiver. Finally, the *signal-to-noise ratio* (*SNR*) is calculated by comparing the received constellation to the transmitted signal. The *SNR* is defined as, $SNR = \mathrm{E}[|X|^2] / \mathrm{E}[|Y - X|^2]$ where X and Y represent the transmitted and received symbols post-equalization, respectively, and E[.] denotes the expectation operator. Since the number of interfering terms due to modal coupling can be interpreted through the MISO equalizers array size, this array size is varied to analyze the reduction in equalization complexity for elliptical core fibers. The normalized MISO complexity required to achieve a given *SNR* for all the modes is given by $(\sum_n MISO\ size_n / N^2)$, which is sum of MISO size required per mode normalized by full MIMO complexity, which is (90×90) in this case. Each mode can have different equalization requirements for a given *SNR*.

A. All-mode transmission

First, we consider a scenario where all the polarization modes are transmitted and received. The MISO array size varies from 1 (SISO) to the total number of polarization modes (90). The MISO array size increases by adding the terms to the equalizer that contributes the most to the crosstalk experienced by the mode under analysis. Interfering modes can be from the same mode group or adjacent mode groups, referred to as the worst interferers. Please note that the worst mode interferers are recalculated for every fiber transmission, as the channel conditions changes. In this analysis, we assume that the channel estimation is available to the receiver. In the scenarios where channels are stable, the worst interferers algorithm can be effectively applied with infrequent recalculations. On the other hand, if the channel decorrelates over time due to environmental perturbations, then the channel estimation must be updated periodically for the algorithm to remain effective. Fig. 11 shows the MISO size required for each transmitted mode to achieve an *SNR* of 28 dB for different ovality values. These are arranged in ascending order against the mode index, for easy understanding. The maximum achievable *SNR,* corresponding to an *OSNR* of 35 dB, is 31 dB, and we focus on cases where the required *SNR* is below this maximum. The results averaged over 500 fiber transmissions by varying the fiber channel conditions, showing that the MISO size required per mode decreases as the ovality increases from 0 to 11.7 %. The average maximum reduction in MISO complexity with optimum ovality compared to circular fibers is 1.89*x* times for an achievable *SNR* of 28 dB.

Fig. 12 illustrates the achievable *SNR* for each mode by increasing the normalized MISO complexity for different ovality values. The normalized MISO complexity varies by varying the target *SNR* for each mode. Achievable *SNR* is the average *SNR* obtained post-equalization for the modes with the calculated MISO array size required per mode to obtain a target *SNR*. As the number of interferers increases, the achievable *SNR* increases with an increase in equalization complexity. For the mode group interferers case where the MIMO of order of mode group is employed for each mode group as in the MGDM system (described in [16]), the average achievable *SNR* is approximately 12.5 dB, as shown by circle marker in Fig. 12. This value remains constant across different ovality levels, because it is fixed to the mode group structure of the circular fibre (undeformed) corresponding to the elliptical fibre under study. This *SNR* is lower than that of the circular fibers for the same MISO complexity, given that equalization is performed by increasing the MISO array size based on the inputs to equalizer as the interferers with the maximum crosstalk. This is due to the non-homogeneous nature of crosstalk as shown in Fig. 3 (a), and the worst mode interferer might be outside the mode group, as a result, use of MIMO equalizer of the mode group order may not always be an optimal approach. Further, elliptical fibers are shown to reduce intra-mode group crosstalk, and they also reduce the number of interfering terms from inter-mode groups, thereby higher *SNR* is achieved at the lower complexity. EC-MMF along with the worst interferes equalization scheme at the receiver, reduces the equalization complexity by 3.9*x* times to achieve the *SNR* as obtained by applying the MIMO of the mode group order size. At higher

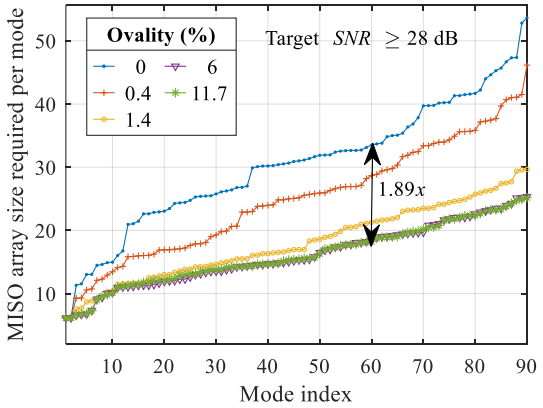

Fig. 11. MISO array required per mode to achieve a target *SNR* of 28 dB when all modes are launched in fiber. Averaged over 500 transmissions by varying the azimuthal displacement and polarization rotation, and channel noise conditions for each fiber section.

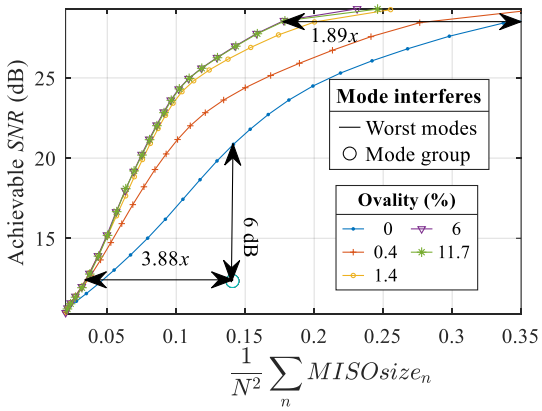

Fig. 12. Achievable *SNR* averaged over all modes by increasing the MISO complexity for a 90-polarization mode fiber. Averaged over 500 transmissions by varying the azimuthal displacement and polarization rotation, and channel noise conditions for each fiber section.

This article has been accepted for publication in Journal of Lightwave Technology. This is the author's version which has not been fully edited and content may change prior to final publication. Citation information: DOI 10.1109/JLT.2025.3603881

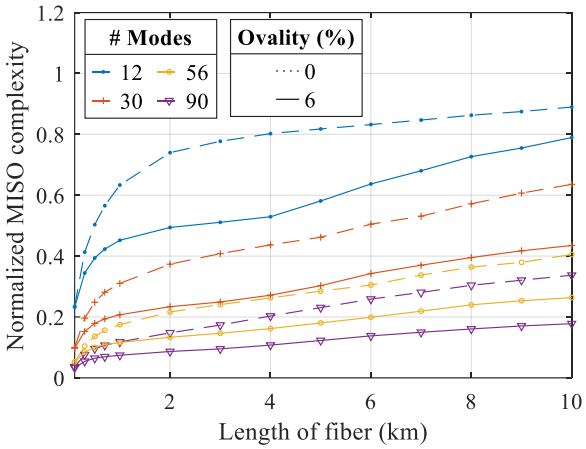

Fig. 13. Normalized MISO complexity required to achieve a target *SNR* of 28 by varying the length of the fiber, for different modes supported in the fiber. Averaged over 500 fiber transmissions by varying the azimuthal displacement and polarization rotation, and channel noise conditions for each fiber section.

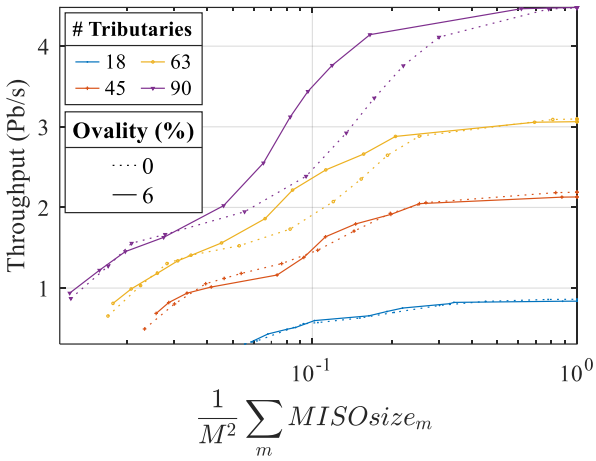

Fig. 14 Throughput for a 90 (*N*) polarization mode 10 km fiber by varying the normalized MISO complexity by transmitting *M* tributaries ($N \geq M$). Averaged over 500 fiber transmissions by varying the azimuthal displacement and polarization rotation, and channel noise conditions for each fiber section.

SNR values, the reduction in MISO complexity is large compared to smaller *SNR* values, to achieve a 20 dB *SNR* the reduction in complexity is 1.74*x*.

Further, we analyze the equalization requirement by varying the length of fiber for different number of modes supported in the fiber. Fig. 13 shows the normalized MISO complexity required for the given fiber to achieve a target *SNR* of 28 dB with crosstalk strength as - 20 dB/km for distances from 100 m to 10 km for circular fibers and an elliptical core fiber with an ovality of 6 %, this ovality is chosen as it is in between the identified optimum range in section III-C. It can be observed that elliptical fibers reduce equalization complexity for all lengths of the fiber and different number of modes supported in the fiber, with an application to intra-datacenter and inter-datacenters links. Maximum reduction is observed from a 12 polarization-mode fiber for 4 km length, beyond this point the complexity gap between circular and elliptical core fiber begins to narrow, due to the increasing contribution of the inter-mode crosstalk in the link. In circular fibers, the intra-mode group crosstalk increases with the mode group order, which becomes more significant as the number of modes increases in the fiber. Therefore, for the fibers supporting the modes from 30 to 90, the decrease in complexity with EC-MMF is increasing with the length up to 10 km, as the intra-mode group crosstalk dominates in the link.

B. Modes with minimum interferers transmission

In this section, we explore the concept of using modes with the minimum number of interferers for data transmission, thereby reducing the number of tributaries used compared to the maximum number of modes supported in the fiber. This results in a lower transmission capacity than could be achieved by fully utilizing all the spatial tributaries. However, this approach may be advantageous when limited infrastructure for transceivers is available; specifically, when the number of transceivers required for maximum capacity cannot be deployed. Here, tributaries refer to the individual data channels that account for the total data carrying capacity of a link. The tributaries are selected based on the power coupling matrix, ensuring that the modes with 99 % of the total power requiring the least number of interferes are chosen for transmission. The ASE noise is added similarly to the all-mode transmission scenario, maintaining an *OSNR* of 35 dB for each transmitted tributaries by applying the same noise level across all the modes. Each transmitted mode experiences the same modal coupling as used during tributary selection, assuming the channel remains stable over time. At the receiver, only the modes carrying data are detected, and equalization is performed as in the all-mode transmission scenario. The MISO array size is varied by incrementally adding the worst interferers for each mode. The equalized *SNR* is then calculated at the receiver for different number of transmitted tributaries (*M*) for a 90-polarization mode fiber. The obtained *SNR* values are then used to find the total throughput of channel occupying a spectral bandwidth (*BW*) of 5 THz over the C-band, neglecting the effect of degradation in *SNR* from wavelength multiplexed channels. Throughput is calculated as,

$$Throughput = BW \sum_{i=1}^{M} (1 + SNR_i) \quad (5)$$

where SNR_i denotes the equalized *SNR* of the i^{th} tributary. Fig. 14 shows the throughput at the receiver versus the normalized MISO complexity per tributary ($\sum_m MISO\ size_m / M^2$, where *M* denotes the number of tributaries) for different number of launched tributaries in circular and elliptical core fibers. It can be observed that the throughput increases sub-linearly with the increase in the normalized MISO complexity before saturating. This trend suggests that full MIMO complexity is not always necessary; by intelligently selecting modes with fewer interferers at the transmitter, a sub-optimal yet high throughput can be achieved with significantly lower receiver complexity. The modes can be intelligently excited selectively using spatial light modulators and the authors in [17] have shown a method to estimate the full channel with less number of tributaries, this makes the approach practical. It has been observed that with the elliptical core fibers (6 % ovality) the maximum throughput is achieved with a lesser complexity at the receiver for the tributaries greater than or equal to 45 compared to circular fibers. This highlights that effective index separation between modes within the mode group in elliptical core fiber reduces modal interference and achieves higher throughput at reduce equalization complexity.

This article has been accepted for publication in Journal of Lightwave Technology. This is the author's version which has not been fully edited and content may change prior to final publication. Citation information: DOI 10.1109/JLT.2025.3603881

C. *Impact of MDL on equalization requirements*

In this subsection, to understand the implications of *MDL* on MIMO equalization, we simulated a 10 km transmission over a fiber supporting 90-polarization modes with a XT = - 20 dB/km by incorporating the total attenuation as described in section III-E distributed over a 1 km fiber length, along with linear mode coupling and other effects in each fiber section. The cabling bending radius in deployed fibers is typically 10*x* the cable diameter, which can be more than 21 cm [50]. Therefore, first we consider all mode data transmission scenario with a bending radius of 90 mm and Fig. 15 shows the MISO equalization requirements to achieve a target *SNR* of 28 dB by transmitting all the modes, in the presence and absence of *MDL* for circular and elliptical core fibers. The results show that the MISO equalization requirements in the presence of *MDL* remain nearly same to the one in absence of *MDL*, for both circular and elliptical core fibers. This finding is valid for the low-to-moderate *MDL* under the assumption that channel estimation is available at the receiver. Please note that the target *SNR* is less than the maximum *SNR*. Higher *SNRs* will have slightly degraded performance in the presence of *MDL*. The degradation in the performance is larger for higher number of modes in the fiber [13].

Also, it is important to note that *MDL* makes the channel matrix non-unitary, which introduces errors in channel estimation when linear equalizers are used. One technique to address this is successive interference cancellation (SIC), where higher-gain modes are decoded first and their interference is cancelled sequentially before decoding weaker modes. As reported in [51], SIC increases complexity by 1.8*x* complexity relative to MMSE in cyclic prefix implementations, and up to 2.6*x* in frequency-domain overlap-save configurations. However, this increase in complexity applies to both circular and elliptical core fibers, keeping their relative equalization requirements unchanged.

Furthermore, when the bending radius is reduced below 60 mm for circular fibers and below 90 mm for elliptical core fibers, the last mode group exhibits *MBL* higher than 0.1 dB for 100 turns, as shown in Fig. 9 (a). Due to mode coupling, this also affects the performance in the other mode groups. In such cases, *MDL* negatively impacts system performance even when SIC is used. In weak-to-intermediate coupling regimes, insufficient mode mixing prevents effective averaging of modal disparities. In contrast to strong coupling regimes, where high mode mixing helps distribute attenuation evenly, SIC cannot overcome *MDL* when mode gain imbalance is significant in weak-to-intermediate coupling regimes. As shown in [51], a two-mode single-mode fiber (SMF) systems under weak coupling, suffers up to 12% loss in achievable information rates was reported at 15,000 km, even with SIC, due to persistent imbalance. Therefore, in such scenarios, a practical and effective strategy is to exclude the lossy last mode group for data transmission [25], which suffers dominant loss due to poor confinement and higher bending losses, thereby improving the condition number of the transmission matrix and allowing SIC (or even linear equalizers) to operate with improved robustness. This will reduce the channel throughput compared to the all-mode transmission, but channel estimation remains feasible. The effective channel matrix $\mathbf{H}_{\mathbf{eff}}(\omega)$ is a reduced-dimension version of $\mathbf{H}(\omega)$, mapping only the actively transmitted modes as described in [17]. Hence, we calculate the MISO equalization requirements to achieve a target *SNR* of 28 dB for a bending radius of 30 mm (which is a standard bending radius for single-mode fibers) by transmitting the data in all the modes excluding the last mode group. From Fig. 15, it can be observed that the required MISO size remains approximately same as without *MDL* for both circular and elliptical core fibers for a 90-polarization mode fiber. Although, the channel estimation complexity increases with *MDL*, but the relative equalization complexity remains same.

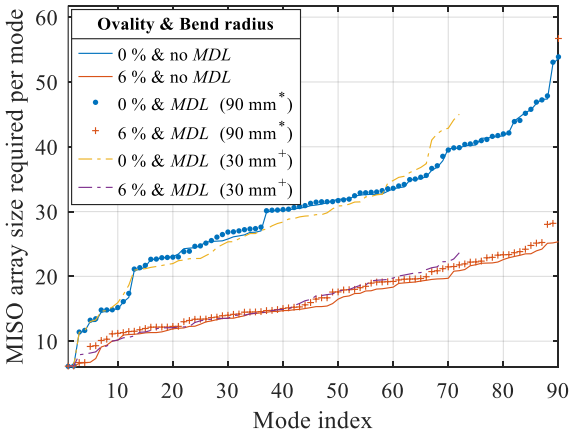

Fig. 15. MISO array requirement per mode to achieve a target *SNR* of 28 dB for the fiber supporting 90-polarization modes. Results are shown for three conditions: without *MDL*, with *MDL* for a bending radius of 90 mm (* - including all mode groups), and with *MDL* bending radius for a 30 mm ($^{+}$- excluding the last mode group). Averaged over 100 transmissions by varying the azimuthal displacement and polarization rotation, and channel noise conditions for each fiber section.

V. Conclusion

This paper presents a comprehensive study on the design and theory of elliptical core graded-index multimode fibers. We demonstrate that EC-MMF offers significant advantages over conventional circular core fibers, including a six-fold reduction in intra-mode group delay and an 11 dB decrease in intra-mode group crosstalk for a 10 km long fiber with crosstalk strength - 20 dB/km, while preserving the minimal delay spread of 35 ps/km for a 90-polarization mode fiber. An optimal ovality range is identified based on the effective indices of the supported modes, providing a useful guideline for fiber manufacturers. We propose an analytical expression for the maximum allowable ovality to minimize intra-mode group crosstalk and validate it through numerical simulations. This expression is extendable to a higher number of fiber modes, and the results show strong agreement with effective index analysis. In addition, we demonstrate that the EC-MMF design enables a reduction in receiver equalization complexity by at least 1.89 times compared to circular core fibers in 10 km data transmission, achieving a signal-to-noise ratio of 28 dB. We also propose a novel transmission method that selects modes with minimal interference. This method shows that sub-optimal throughput can be achieved at reduced equalization complexity than the full MIMO complexity, especially in elliptical core fibers under constrained transceiver deployment, providing a significant efficiency boost for multimode SDM

systems. Further, MISO equalization requirements remain approximately unchanged in the presence of *MDL* for a bending radius of 30 mm to achieve a target *SNR* of 28 dB, provided the channel estimation is available and highly lossy mode groups are excluded from the transmission. Finally, for a fiber supporting 90-polarization modes, data transmission using all the modes is feasible for circular fibers between bending radius of 60 mm to 90 mm, whereas for elliptical core fibers, it is preferable to exclude the last mode group for data transmission when bending radius are below 90 mm due to high *MDL*, which is the similar to circular fibres below 60 mm. Overall, our findings offer a promising pathway to develop low-complexity, high-capacity multimode SDM systems for intra-data center and inter-data center applications.

VI. Appendix I: Analytical Expression of Maximum Ovality

To determine the maximum ovality, effective index variation with ovality of modes plays a crucial role as discusses in section III-A. The effective index of an LP_{mn} mode in a graded-index circular core fiber, under the weakly guiding approximation and neglecting birefringence effects, is given by the following expression [18]:,

$$n_{eff}(w_1, LP_{mn}) = \frac{1}{kw_1}\{(kw_1 n_{co})^2 - \tilde{B}(w_1, LP_{mn})^2\}^{\frac{1}{2}} \tag{6}$$

where k is the wavenumber, w_1 is the core radius, and n_{co} is the core index. The term $\tilde{B}(w_1, LP_{mn})$ is a function dependent on the core radius, mode group and graded exponent α, and is expressed as:

$$\tilde{B}(w_1, LP_{mn}) = \left\{\frac{\Gamma\left(\frac{1}{\alpha}+\frac{1}{2}\right)(\alpha+2)(m+2n-1)\pi^{\frac{1}{2}}V(w_1)^{\frac{2}{\alpha}}}{2\Gamma\left(\frac{1}{\alpha}\right)}\right\}^{\frac{\alpha}{\alpha+2}} \tag{7}$$

Here, the V-number of the fiber for a radius w_1 is given by $V(w_1) = kw_1 n_{co}\sqrt{2\Delta n_{co}}$, and Δn_{co} is the relative core-clad index difference and the gamma function is given by,

$$\Gamma(z) = \int_0^\infty t^{z-1}e^{-t}dt \tag{8}$$

In Equation (6), it is assumed that all modes within the same mode group have the same effective index because the term $(m+2n-1)$ corresponds to the mode group order. Importantly, this assumes the ideal mode pattern does not change with the graded exponent α [52]. Additionally, in elliptical core fibers, as ovality increases, the semi-major axis length increases, leading to an increase in the effective indices of a given mode group when considering the radius as major axis ($w_1 = a_x(\chi)$). Conversely, when considering the semi-minor axis as the radius ($w_1 = a_y(\chi)$), the effective indices decrease. Here, the effective area of the fiber is also changing with the core-radius as both the radius are changing independent of each other, whereas in the numerical results discussed in section III-A, we have maintained the core area constant, like the circular fibers. Therefore, the slope of the effective index obtained here with ovality is different from the one obtained in Fig. 4 (b). It is important to note that the effective index in this analysis is derived using the WKB theory, which differs from the exact solution based on the vector field equations as discussed in [10]. The maximum permissible ovality for a multimode fiber to minimize intra-mode group crosstalk occurs at the intersection point of the effective index of the penultimate mode group considering the radius as the minor axis and the effective index of the last mode group considering the radius as the major axis. Considering the total number of mode groups supported in the fiber is given by N_{mg}, $(m+2n-1)$ indices of the penultimate mode group and for the last mode group are given by $(N_{mg}-1)$ and N_{mg} respectively, and maximum ovality can be expressed mathematically as,

$$\chi_{\max,\text{ana}} = \chi\{[n_{\text{eff,minor}}(a_y(\chi), LP_{mn} \in (N_{\text{mg}}-1)) - n_{\text{eff,major}}(a_x(\chi), LP_{mn} \in N_{\text{mg}})] = 0\} \tag{9}$$

Substituting the values of respective effective indices using Eqn. (6) in Eqn. (9),

$$\begin{aligned}\frac{1}{ka_y(\chi_{max,ana})}&\left[(ka_y(\chi_{max,ana})n_{co})^2 - \widetilde{B^2}(a_y(\chi_{max,ana}), LP_{mn} \in (N_{\text{mg}}-1))\right]^{\frac{1}{2}} \\ &= \frac{1}{ka_x(\chi_{max,ana})}\left[(ka_x(\chi_{max,ana})n_{co})^2 - \widetilde{B^2}(a_x(\chi_{max,ana}), LP_{mn} \in N_{\text{mg}})\right]^{\frac{1}{2}}\end{aligned} \tag{10}$$

Upon simplifying and canceling terms in Eqn. (10), we obtain,

$$\frac{\tilde{B}(a_y(\chi_{max,ana}), LP_{mn} \in (N_{\text{mg}}-1))}{\tilde{B}(a_x(\chi_{max,ana}), LP_{mn} \in N_{\text{mg}})} = \frac{a_y(\chi_{max,ana})}{a_x(\chi_{max,ana})} \tag{11}$$

From Eqn. (7), $\tilde{B}(a_x(\chi_{max,ana}), LP_{mn} \in N_{\text{mg}})$ and $\tilde{B}(a_y(\chi_{max,ana}), LP_{mn} \in (N_{\text{mg}}-1))$ can be obtained and substituting these values in Eqn. (11) and solving we get,

$$\left(\frac{(N_{mg}-1)\,V\left(a_y(\chi_{max,ana})\right)^{\frac{2}{\alpha}}}{(N_{mg})\,V\left(a_x(\chi_{max,ana})\right)^{\frac{2}{\alpha}}}\right)^{\frac{\alpha}{\alpha+2}} = \frac{a_y(\chi_{max,ana})}{a_x(\chi_{max,ana})} \tag{12}$$

Further substituting V values and solving the above equation,

$$\left(\frac{(N_{mg}-1)}{N_{mg}}\left(\frac{a_y(\chi_{max,ana})}{a_x(\chi_{max,ana})}\right)^{\frac{2}{\alpha}}\right)^{\frac{\alpha}{\alpha+2}} = \frac{a_y(\chi_{max,ana})}{a_x(\chi_{max,ana})} \tag{13}$$

Solving Eqn. 13, we get

$$\left\{\frac{N_{mg}-1}{N_{mg}} = \frac{2-\chi_{max,ana}}{2+\chi_{max,ana}}\right\} \tag{14}$$

and further simplifying, we obtain Eqn. (3). From Eqn. 3, it is observed that the maximum analytical ovality value is independent of the fiber core parameters, as these parameters remain constant across all the mode groups. This analytical approach provides a method that can be used for calculating the maximum ovality for optimal performance, without needing to compute the actual effective indices for each mode group. As shown in Fig. 5, analytical values coincide with the numerical values.

VII. Acknowledgment

The authors acknowledge Prof. Polina Bayvel and the reviewers for the comments on the paper. The authors acknowledge the use of the UCL Myriad High Performance Computing Facility (Myriad@UCL), and associated support services, in the completion of this work. To access the underlying data for this publication, see: https://doi.org/10.5522/04/25681374.

REFERENCES

[1] D. J. Richardson, J. M. Fini, and L. E. Nelson, "Space-division multiplexing in optical fibres," *Nature Photonics,* vol. 7, p. 354, 2013, doi: 10.1038/nphoton.2013.94.

[2] R.-J. Essiambre and R. W. Tkach, "Capacity Trends and Limits of Optical Communication Networks," *Proceedings of the IEEE,* vol. 100, no. 5, pp. 1035-1055, 2012, doi: 10.1109/jproc.2012.2182970.

[3] G. Li, N. Bai, N. Zhao, and C. Xia, "Space-division multiplexing: the next frontier in optical communication," *Adv. Opt. Photon.,* vol. 6, no. 4, pp. 413-487, 2014/12/31 2014, doi: 10.1364/AOP.6.000413.

[4] P. J. Winzer, "Making spatial multiplexing a reality," *Nature Photonics,* vol. 8, no. 5, pp. 345-348, 2014/05/01 2014, doi: 10.1038/nphoton.2014.58.

[5] P. J. Winzer and D. T. Neilson, "From Scaling Disparities to Integrated Parallelism: A Decathlon for a Decade," *J. Lightw. Technol.,* vol. 35, no. 5, pp. 1099-1115, 2017, doi: 10.1109/JLT.2017.2662082.

[6] W. Klaus, P. J. Winzer, and K. Nakajima, "The Role of Parallelism in the Evolution of Optical Fiber Communication Systems," *Proceedings of the IEEE,* vol. 110, no. 11, pp. 1619-1654, 2022, doi: 10.1109/JPROC.2022.3207920.

[7] F. M. Ferreira, C. S. Costa, S. Sygletos, and A. D. Ellis, "Semi-analytical modelling of linear mode coupling in few-mode fibers," *Journal of Lightwave Technology,* 7 2017, doi: 10.1109/JLT.2017.2727441.

[8] C. S. Costa, F. M. Ferreira, N. M. Suibhne, S. Sygletos, and A. D. Ellis, "Receiver Memory Requirement in Mode Delay Compensated Few-Mode Fibre Spans with Intermediate Coupling," in *ECOC 2016; 42nd European Conference on Optical Communication*, 18-22 Sept. 2016 2016, pp. 1-3.

[9] R. Maruyama, N. Kuwaki, S. Matsuo, and M. Ohashi, "Relationship Between Mode Coupling and Fiber Characteristics in Few-Mode Fibers Analyzed Using Impulse Response Measurements Technique," *Journal of Lightwave Technology,* vol. 35, no. 4, pp. 650-657, 2017, doi: 10.1109/JLT.2016.2609002.

[10] K.-P. Ho and J. M. Kahn, "Mode Coupling and its Impact on Spatially Multiplexed Systems," pp. 491-568, 2013, doi: 10.1016/b978-0-12-396960-6.00011-0.

[11] A. A. Juarez, E. Krune, S. Warm, C. A. Bunge, and K. Petermann, "Modeling of Mode Coupling in Multimode Fibers With Respect to Bandwidth and Loss," *Journal of Lightwave Technology,* vol. 32, no. 8, pp. 1549-1558, 2014, doi: 10.1109/JLT.2014.2308059.

[12] B. Inan *et al.*, "DSP complexity of mode-division multiplexed receivers," *Opt. Express,* vol. 20, no. 10, pp. 10859-10869, 2012/05/07 2012, doi: 10.1364/OE.20.010859.

[13] F. M. Ferreira and F. A. Barbosa, "Maximizing the Capacity of Graded-Index Multimode Fibers in the Linear Regime," *Journal of Lightwave Technology,* vol. 42, no. 5, pp. 1626-1633, 2024, doi: 10.1109/JLT.2023.3324611.

[14] B. Franz and H. Bulow, "Mode group division multiplexing in graded-index multimode fibers," *Bell Labs Technical Journal,* vol. 18, no. 3, pp. 153-172, 2013, doi: 10.1002/bltj.21632.

[15] A. Gatto *et al.*, "Partial-MIMO based Mode-Group transmission and routing in a field-deployed 15-mode network: throughput, DSP resources and network flexibility," *Journal of Lightwave Technology,* pp. 1-13, 2024, doi: 10.1109/JLT.2024.3383290.

[16] P. Boffi *et al.*, "Mode-Group Division Multiplexing: Transmission, Node Architecture, and Provisioning," *Journal of Lightwave Technology,* vol. 40, no. 8, pp. 2378-2389, 2022, doi: 10.1109/JLT.2021.3135636.

[17] F. A. Barbosa and F. M. Ferreira, "On a Scalable Path for Multimode SDM Transmission," *Journal of Lightwave Technology,* 2023.

[18] M. B. Shemirani, W. Mao, R. A. Panicker, and J. M. Kahn, "Principal Modes in Graded-Index Multimode Fiber in Presence of Spatial- and Polarization-Mode Coupling," *Journal of Lightwave Technology,* vol. 27, no. 10, pp. 1248-1261, 2009, doi: 10.1109/jlt.2008.2005066.

[19] A. Vijay and J. M. Kahn, "Effect of Higher-Order Modal Dispersion in Direct-Detection Mode-Division-Multiplexed Links," *Journal of Lightwave Technology,* vol. 41, no. 6, pp. 1670-1683, 2023, doi: 10.1109/JLT.2022.3226704.

[20] J. Liu *et al.*, "1-Pbps orbital angular momentum fibre-optic transmission," *Light: Science & Applications,* vol. 11, no. 1, p. 202, 2022/07/05 2022, doi: 10.1038/s41377-022-00889-3.

[21] M. Banawan *et al.*, "Using Standard 2×2 MIMO to Increase Capacity of Spatial Multiplexing with OAM Modes," *Journal of Lightwave Technology,* vol. 41, no. 7, pp. 1974-1984, 2023/04/01 2023..

[22] K. Ingerslev *et al.*, "12 mode, WDM, MIMO-free orbital angular momentum transmission," *Opt. Express,* vol. 26, no. 16, pp. 20225-20232, 2018/08/06 2018, doi: 10.1364/OE.26.020225.

[23] N. Bozinovic *et al.*, "Terabit-Scale Orbital Angular Momentum Mode Division Multiplexing in Fibers," *Science,* vol. 340, no. 6140, pp. 1545-1548, 2013, doi: doi:10.1126/science.1237861.

[24] A. E. Willner *et al.*, "Optical communications using orbital angular momentum beams," *Adv. Opt. Photon.,* vol. 7, no. 1, pp. 66-106, 2015/03/31 2015, doi: 10.1364/AOP.7.000066.

[25] G. Milione *et al.*, "MIMO-less space division multiplexing with elliptical core optical fibers," in *Optical Fiber Communication Conference*, 2017: Optica Publishing Group, p. Tu2J. 1.

[26] E. Ip *et al.*, "SDM transmission of real-time 10GbE traffic using commercial SFP + transceivers over 0.5km elliptical-core few-mode fiber," *Opt. Express,* vol. 23, no. 13, pp. 17120-17126, 2015/06/29 2015, doi: 10.1364/OE.23.017120.

[27] M. Li, X. Li, H. Li, and W. Zhang, "Bow-tie holes-aided elliptical-core polarization-maintaining fiber with high birefringence," *Optical Fiber Technology,* vol. 73, p. 103073, 2022.

[28] A. Corsi, J. Ho Chang, R. Wang, L. Wang, L. Ann Rusch, and S. LaRochelle, "Highly elliptical core fiber with stress-induced birefringence for mode multiplexing," *Opt. Lett.,* vol. 45, no. 10, pp. 2822-2825, 2020.

[29] S. Sakpal *et al.*, "Stability of Ince–Gaussian beams in elliptical core few-mode fibers," *Opt. Lett.,* vol. 43, no. 11, pp. 2656-2659, 2018/06/01 2018, doi: 10.1364/OL.43.002656.

[30] A. M. Velázquez-Benítez *et al.*, "Scaling photonic lanterns for space-division multiplexing," *Scientific Reports,* vol. 8, no. 1, p. 8897, 2018, doi: 10.1038/s41598-018-27072-2.

[31] N. K. Fontaine *et al.*, "Hermite-Gaussian mode multiplexer supporting 1035 modes," in *2021 Optical Fiber Communications Conference and Exhibition (OFC)*, 6-10 June 2021 2021, pp. 1-3.

[32] N. K. Fontaine, R. Ryf, H. Chen, D. T. Neilson, K. Kim, and J. Carpenter, "Laguerre-Gaussian mode sorter," *Nature Communications,* vol. 10, no. 1, p. 1865, 2019/04/26 2019, doi: 10.1038/s41467-019-09840-4.

[33] A. Antikainen, R.-J. Essiambre, and G. P. Agrawal, "Determination of modes of elliptical waveguides with ellipse transformation perturbation theory," *Optica,* vol. 4, no. 12, pp. 1510-1513, 2017/12/20 2017, doi: 10.1364/OPTICA.4.001510.

[34] G. Milione, E. Ip, M. J. Li, J. Stone, G. Peng, and T. Wang, "Spatial mode analysis of an elliptical-core, few-mode, optical fiber for MIMO-less space-division-multiplexing," in *2016 Optical Fiber Communications Conference and Exhibition (OFC)*, 20-24 March 2016 2016, pp. 1-3.

[35] G. Milione, E. Ip, M.-J. Li, J. Stone, G. Peng, and T. Wang, "Mode crosstalk matrix measurement of a 1 km elliptical core few-mode optical fiber," *Optics Letters,* vol. 41, no. 12, pp. 2755-2758, 2016/06/15 2016, doi: 10.1364/OL.41.002755.

[36] F. Parmigiani, Y. Jung, L. Grüner-Nielsen, T. Geisler, P. Petropoulos, and D. J. Richardson, "Elliptical Core Few Mode Fibers for Multiple-Input Multiple Output-Free Space Division Multiplexing Transmission," *IEEE Photonics Technology Letters,* vol. 29, no. 21, pp. 1764-1767, 2017, doi: 10.1109/LPT.2017.2740499.

[37] G. Peng and M. J. Li, "Elliptical core multimode optical fibers," in *2012 17th Opto-Electronics and Communications Conference*, 2-6 July 2012 2012, pp. 485-486, doi: 10.1109/OECC.2012.6276534.

[38] R. Yadav, F. Barbosa, M.-J. Li, and F. Ferreira, *Enabling multimode SDM at reduced equalization complexity via optimized elliptical core fibers* (OPTO). SPIE, 2025.

[39] K. F. Barrell and C. Pask, "Geometric optics analysis of non-circular, graded-index fibres," *Optical and Quantum Electronics,* vol. 11, no. 3, pp. 237-251, 1979/05/01 1979, doi: 10.1007/BF00620110.

[40] C. Yeh, "Modes in weakly guiding elliptical optical fibres," *Optical and Quantum Electronics,* vol. 8, no. 1, pp. 43-47, 1976/01/01 1976, doi: 10.1007/BF00620439.

[41] C. Yeh, "Elliptical dielectric waveguides," *Journal of Applied Physics,* vol. 33, no. 11, pp. 3235-3243, 1962.

[42] D. Gloge, "Weakly Guiding Fibers," *Appl. Opt.,* vol. 10, no. 10, pp. 2252-2258, 1971/10/01 1971, doi: 10.1364/AO.10.002252.

[43] A. B. Fallahkhair, K. S. Li, and T. E. Murphy, "Vector Finite Difference Modesolver for Anisotropic Dielectric Waveguides," *Journal of Lightwave Technology,* vol. 26, no. 11, pp. 1423-1431, 2008, doi: 10.1109/JLT.2008.923643.

[44] J. Noda, K. Okamoto, and Y. Sasaki, "Polarization-maintaining fibers and their applications," *Journal of Lightwave Technology,* vol. 4, no. 8, pp. 1071-1089, 1986, doi: 10.1109/JLT.1986.1074847.

[45] R. Yadav, F. A. Barbosa, and F. M. Ferreira, "Modal Dynamics for Space-Division Multiplexing in Multi-Mode Fibers," *Journal of Lightwave Technology,* pp. 1-9, 2024, doi: 10.1109/JLT.2024.3365307.

[46] X. Chen, M.-J. Li, J. Koh, A. Artuso, and D. A. Nolan, "Effects of bending on the performance of hole-assisted single polarization fibers," *Opt. Express,* vol. 15, no. 17, pp. 10629-10636, 2007/08/20 2007, doi: 10.1364/OE.15.010629.

[47] R. T. Schermer and J. H. Cole, "Improved Bend Loss Formula Verified for Optical Fiber by Simulation and Experiment," *IEEE Journal of Quantum Electronics,* vol. 43, no. 10, pp. 899-909, 2007, doi: 10.1109/JQE.2007.903364.

[48] M. Ohashi, K. Shiraki, and K. Tajima, "Optical loss property of silica-based single-mode fibers," *Journal of Lightwave Technology,* vol. 10, no. 5, pp. 539-543, 1992, doi: 10.1109/50.136085.

[49] K. Saitoh and M. Koshiba, "Full-vectorial imaginary-distance beam propagation method based on a finite element scheme: application to photonic crystal fibers," *IEEE Journal of Quantum Electronics,* vol. 38, no. 7, pp. 927-933, 2002, doi: 10.1109/JQE.2002.1017609.

[50] Leviton. "PRODUCT SPECIFICATIONS Data Center Plenum with ARMOR-TEK (DAPK12B)." (accessed.

[51] E. S. Chou and J. M. Kahn, "Successive Interference Cancellation on Frequency-Selective Channels With Mode-Dependent Gain," *Journal of Lightwave Technology,* vol. 40, no. 12, pp. 3729-3738, 2022, doi: 10.1109/JLT.2022.3150355.

[52] A. W. Snyder and J. D. Love, "Circular fibers," in *Optical Waveguide Theory*. Boston, MA: Springer US, 1983, pp. 301-335.